Correlation between head shape and volumetric changes following spring-assisted posterior vault expansion

Karan R.R. Ramdat Misier [a, *], Richard W.F. Breakey [b], Lara S. van de Lande [b], Benedetta Biffi [c], Paul G.M. Knoops [b], Silvia Schievano [b, c], Cornelia J.J.M. Caron [a, b], David J. Dunaway [b], Maarten J. Koudstaal [a, b], N.U. Owase Jeelani [b], Alessandro Borghi [b]

[a] Department of Oral and Maxillofacial Surgery, Erasmus University Medical Centre, Dr. Molewaterplein 40, 3015 GD, Rotterdam, the Netherlands
[b] Craniofacial Unit, Great Ormond Street Hospital for Children, Great Ormond Street, London, WC1N 3JH, United Kingdom
[c] UCL Institute of Cardiovascular Science, 30 Guilford St, Holborn, London, WC1N 1EH, United Kingdom

ARTICLE INFO

ABSTRACT

The aim of the study was to investigate whether different head shapes show different volumetric changes following spring-assisted posterior vault expansion (SA-PVE) and to investigate the influence of surgical and morphological parameters on SA-PVE.

Preoperative three-dimensional skull models from patients who underwent SA-PVE were extracted from computed tomography scans. Patient head shape was described using statistical shape modelling (SSM) and principal component analysis (PCA). Preoperative and postoperative intracranial volume (ICV) and cranial index (CI) were calculated. Surgical and morphological parameters included skull bone thickness, number of springs, duration of spring insertion and type of osteotomy.

In the analysis, 31 patients were included. SA-PVE resulted in a significant ICV increase (284.1 ± 171.6 cm^3, $p < 0.001$) and a significant CI decrease ($-2.9 \pm 4.3\%$, $p < 0.001$). The first principal component was significantly correlated with change in ICV (Spearman $\rho = 0.68$, $p < 0.001$). Change in ICV was significantly correlated with skull bone thickness ($\rho = -0.60$, $p < 0.001$) and age at time of surgery ($\rho = -0.60$, $p < 0.001$). No correlations were found between the change in ICV and number of springs, duration of spring insertion and type of osteotomy.

SA-PVE is effective for increasing the ICV and resolving raised intracranial pressure. Younger, brachycephalic patients benefit more from surgery in terms of ICV increase. Skull bone thickness seems to be a crucial factor and should be assessed to achieve optimal ICV increase. In contrast, insertion of more than two springs, duration of spring insertion or performing a fully cut through osteotomy do not seem to impact the ICV increase. When interpreting ICV increases, normal calvarial growth should be taken into account.

1. Introduction

Craniosynostosis is a congenital condition in which one or more cranial sutures fuse prematurely. It can occur in isolated form, in which only one suture is affected; in multisuture or complex form, in which multiple sutures are affected; or as part of a syndrome, in which the isolated or multisuture craniosynostosis presents itself together with other physical abnormalities (Johnson et al., 2011). Syndromic craniosynostosis can be secondary to various syndromes, including Apert, Crouzon, Pfeiffer and Muenke (Renier et al., 2000; Bouaoud et al., 2020). Patients with multisuture synostosis, in which no genetic mutation is found, are classified as complex craniosynostosis patients (Czerwinski et al., 2011).

Patients with complex and syndromic craniosynostosis have a high risk of developing raised intracranial pressure (ICP), which can lead to optic nerve atrophy, visual impairments, hearing loss, breathing and feeding difficulties, and neuro-developmental delay (Taylor et al., 2001; Wiberg et al., 2012; Kim et al., 2019; Lehner

---

* Corresponding author. Department of Oral and Maxillofacial Surgery, Erasmus University Medical Centre, Rotterdam, Dr. Molewaterplein 40, 3015 GD, Rotterdam, the Netherlands.
E-mail address: k.ramdatmisier@erasmusmc.nl (K.R.R. Ramdat Misier).

K.R.R. Ramdat Misier, R.W.F. Breakey, L.S. van de Lande et al.

Journal of Cranio-Maxillo-Facial Surgery 50 (2022) 343—352

et al., 2019; Khonsari et al., 2020). Initial treatment of craniosynostosis aims to enlarge the skull volume, in order to relieve the raised ICP (Renier et al., 2000). A common surgical technique for expanding the skull volume is posterior vault expansion, in which the posterior part of the cranium is surgically expanded (Sgouros et al., 1996). This conventional technique requires large dural dissection, which in turn may result in a high risk of perioperative blood loss. In addition, the amount of expansion achieved by this approach is limited by the tractability of the skin (De Jong et al., 2013). More recently, spring-assisted posterior vault expansion (SA-PVE) has been adopted to overcome these limitations. In this technique, metal springs are used to aid the expansion of the posterior part of the skull, which occurs gradually over a few weeks. The springs allow on-table skin closure, as the devices are initially placed in a compressed state, obviating the limiting factor of skin tractability. Besides easier skin closure, SA-PVE has also been reported to achieve greater expansion compared to the conventional technique (De Jong et al., 2013). The inserted springs are removed in a second procedure (Rtshiladze et al., 2019).

Outcomes of SA-PVE in terms of change in intracranial volume (ICV) and head shape have not been quantitatively analysed before. Conventional morphological parameters to quantify head shape such as the cranial index (CI) (Kolar et al., 1997) and the turricephaly index (TI) (O'Hara et al., 2019) are simplified measurements that do not capture the entirety of head shape information. Statistical shape modelling (SSM) allows three-dimensional (3D) shape analysis of a population of objects, capturing the populations' mean shape and the main modes of shape variation between the objects by means of principal components analysis (PCA). This technique can be used, for example, to describe each object in the shape space with a number, to visually and numerically assess shape differences, and to group similar shapes in different clusters. Every principal component accounts for a certain percentage of the shape variation and can be ordered based on their contribution to shape differences between the objects (Jolliffe, 2002; Durrleman et al., 2014).

The objective of this study was to assess the effect of the preoperative head shape, patient demographics and surgical parameters on surgical outcomes of SA-PVE.

2. Materials and methods

2.1. Patient population

The database of all patients who underwent SA-PVE at the Great Ormond Street Hospital for Children, London, UK, between 2008 and 2018 was reviewed. Patients with pre- and postoperative CT scans with sufficient image quality for calculation of the ICV and bone thickness were included. Pre- and postoperative CT scans of the eligible patients were collected, together with patient demographics and surgical data. The study was approved by the Ethics Committee of the Great Ormond Street Hospital for Children (Ethical approval number: UK REC 15/LO/0386).

2.2. Surgical technique

In SA-PVE, the patient is placed in prone position with the neck in a neutral or slightly flexed position. A coronal incision is made into the subgaleal plane and the skin flap is pushed back caudally. After periosteum stripping, the lines for the bone cuts are fashioned and burr holes are made. The burr holes are connected using a craniotome, making the bone cuts. For safety, the most caudal bone cut usually stops just above the torcula. The posterior bone flap is then pushed back by the surgeon's thumbs, while resting his fingers on the anterior part of the bone cut, to test the mobility of the bone flap and to 'crack' the remaining bone attachments. The flap in the patients in whom full length osteotomy is not performed remains attached to the dura and the periosteum. In those cases where the flap is fully cut through, surgical wires are used to fixate the flap to the rest of the skull. Next, standardised springs (Active Spring Company, Thaxted, UK) (Rodgers et al., 2017) are placed through grooves into the bone along the osteotomy line (Figs. 1 and 2). After placement, the springs are covered under the periosteum followed by closure of the skin (Fig. 3). The choice of type, number and location of springs is based on the surgeon's experience and varies for each case. As few as two springs, one on either side of the head, are placed, in an attempt to limit the amount of foreign material, but up to six springs are placed to guarantee the desired expansion. In Fig. 4, pre- and postoperative soft tissue scans, as well as the clinical situation 1 year after surgery, are displayed.

2.3. Computed tomography image data processing

Digital Imaging and Communications in Medicine (DICOM) images of all CT scans were imported into Simpleware™ ScanIP (Synopsys, Inc., Mountain View, CA, USA), where 3D meshes of the patient skull bone were extracted using a semi-automatic threshold approach. Redundant structures such as draping, the back of the CT scanner or tubes and lines were manually removed. Meshes were imported in Autodesk Meshmixer (Autodesk Research, Toronto, ON, Canada), where further processing was performed. To isolate the region of interest, a planar cut was created in all models, through the nasion and upper border of the external auditory canals (Fig. 5). Voids in the bone models were filled to create a continuous skull surface model for SSM.

2.4. Measurements from CT reconstructions

From the 3D meshes, the following morphological parameters were measured:

- Preoperative and postoperative CI, calculated as the ratio between skull width (measured as the maximum biparietal width of the model) and length (measured as the maximum occipitofrontal length of the model);
- Preoperative skull bone thickness, calculated as the closest point distance of the inner and outer surface of the skull model, using the Vascular Modelling Toolkit (VMTK, Bergamo, Italy) along with Matlab (MathWorks, Natick, MA, USA (Antiga et al., 2008)). This measurement was performed for the upper 75% of the skull, thus excluding the orbits, because of the many bone artefacts in this area. After calculating the distances, the average skull thickness was obtained for each patient;
- ICV, calculated using FSL (FMRIB Analysis Group, Oxford, UK (Breakey et al., 2017; Breakey et al., 2018)) or a semi-automatic approach using Simpleware™ ScanIP, when the automatic method failed to segment the intracranial region of interest. Due to the time difference amongst patients between the preoperative CT scan date and the day of surgery, calculated preoperative ICV values were adjusted to the day of surgery, whilst postoperative values were adjusted to one year after surgery, using the syndrome specific growth curves published by Breakey et al. (Breakey et al., 2018). Percentage change in ICV was calculated variation in ICV divided by the postoperative ICV.

2.5. Statistical shape modelling and principal component analysis

SSM was performed using Deformetrica (www.deformetrica.org), a non-parametric framework, which allows for analysis and
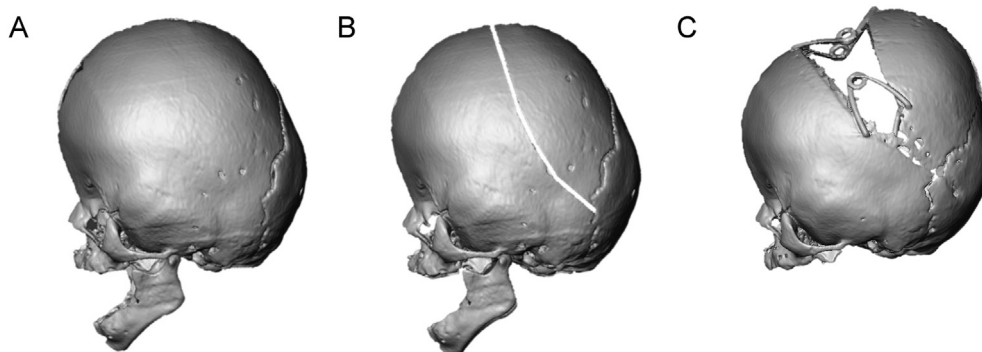
Fig. 1. Illustration of the spring-assisted posterior vault expansion (SA-PVE) process. A: Preoperative model of a SA-PVE patient. B: Visualization of the osteotomy. C: 3D model of the SA-PVE patient with springs inserted.

Fig. 2. Peri-operative image of spring insertion between osteotomy lines.

processing of smooth shapes without the need for landmarking. This is a suitable method for shapes such as the calvarium, which lack evident anatomical landmarks (Durrleman et al., 2014; Rodriguez-Florez et al., 2017a). For SSM and PCA, all preoperative

CT models were scaled to match the average preoperative population ICV, in order to allow the principal components to focus on head shape differences instead of size differences. SSM was used on the preoperative bone models to generate the population 3D preoperative mean head shape (template), and to calculate the individual deformation vector for every patient 3D model from this template (Tenhagen et al., 2016). PCA was performed on these deformation vectors to assess shape differences in the preoperative bone models.

2.6. Surgical parameters

Surgical parameters were extracted and recorded in terms of:

- Type of osteotomies: 'hinge' group, for patients where the calvarial bone remained attached to the posterior skull (Fig. 6A) vs. 'flap' group, for patients with a fully cut through osteotomy (Fig. 6B). Determination of the type of osteotomy was achieved by analysis of the postoperative cephalogram and postoperative CT scan, together with the operating neurosurgeon (NUOJ);
- Number of springs inserted per patient: patients with two springs inserted vs. patients with more than two springs (i.e., either four or six);
- Duration of spring insertion, measured as the time between the spring implantation surgery and the spring removal surgery.
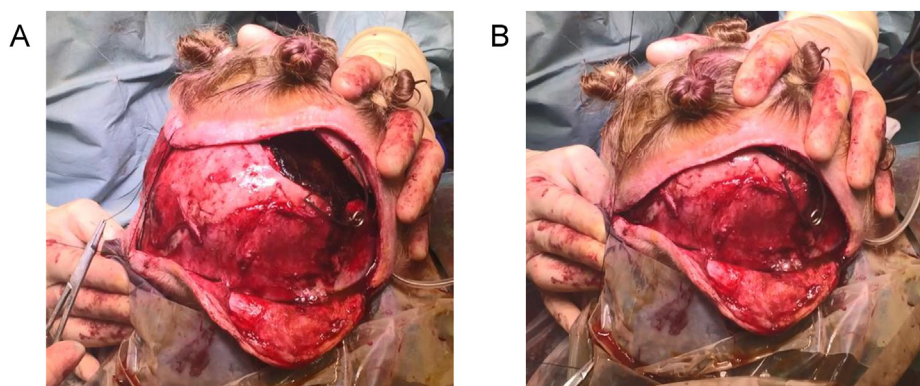

Fig. 3. Demonstration of skin closure with springs in situ. A: Non-compressed spring in situ just before skin closure. B: Closure of the skin is possible because of compression of the spring.
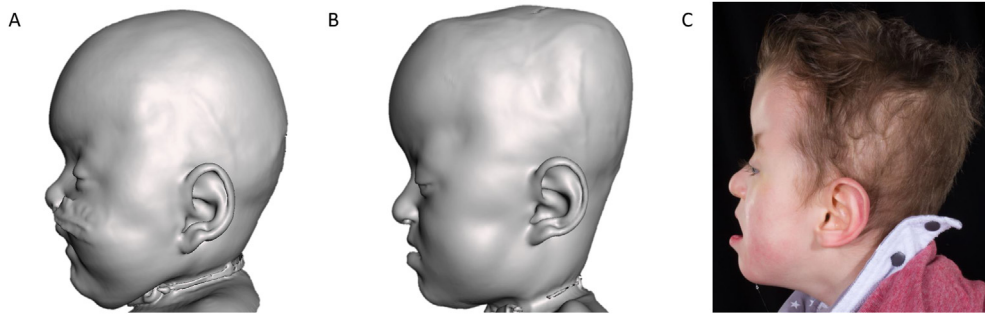
Fig. 4. A: Pre-operative soft tissue model of a spring-assisted posterior vault expansion (SA-PVE) patient. B: Postoperative soft tissue model. C: Clinical photograph 1 year after surgery.
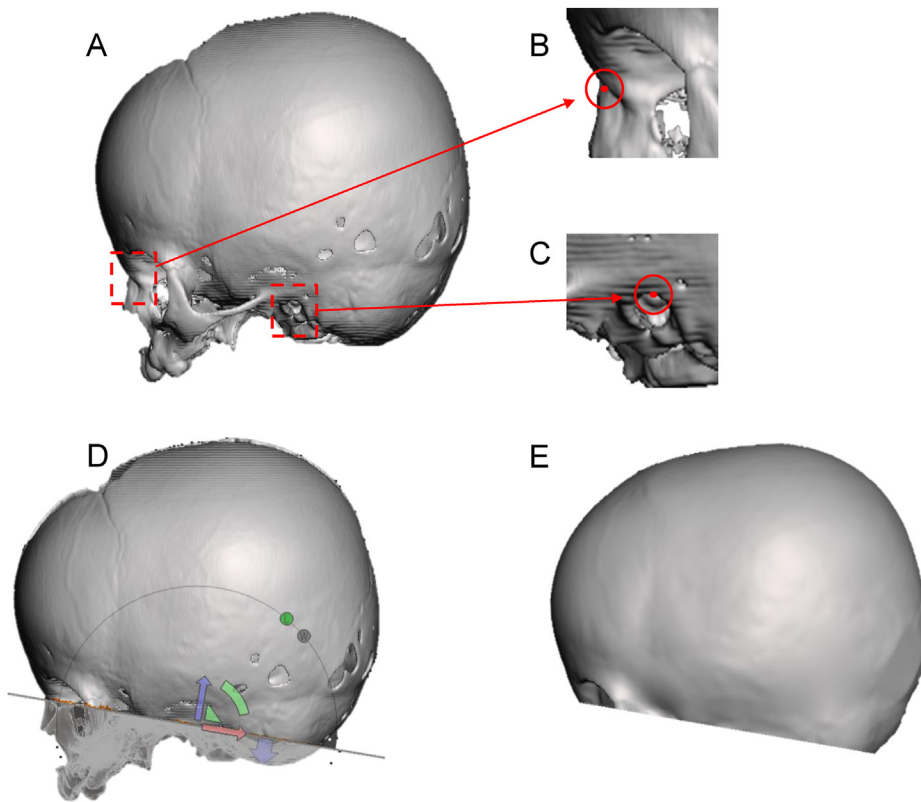

Fig. 5. Planar cut in the bone model. A: Bone model with the nasion (B) and external auditory canal (C) highlighted. D: Cutting plane. E: Final model resulting from the planar cut and filling of voids.
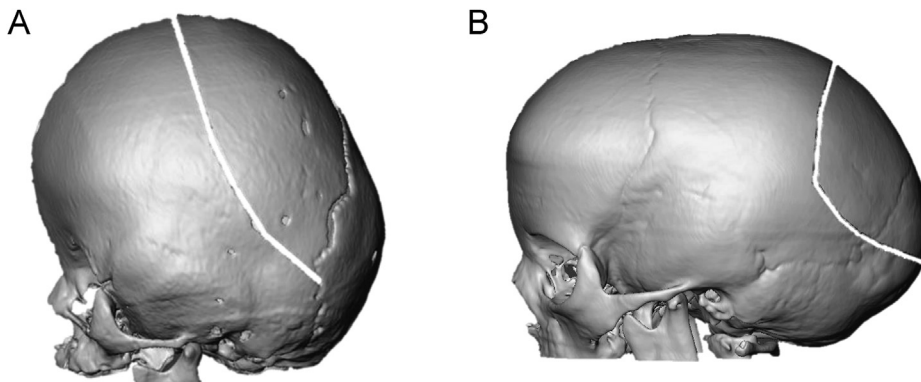

Fig. 6. Types of osteotomies. A: 3D model of a patient with a 'hinge' osteotomy. B: 3D model of a patient with a 'flap' osteotomy.

K.R.R. Ramdat Misier, R.W.F. Breakey, L.S. van de Lande et al.

Journal of Cranio-Maxillo-Facial Surgery 50 (2022) 343−352

2.7. Statistical analysis

Surgical outcomes were correlated with patient demographics, surgical parameters as well as head shape described by PCA (first principal component).

All correlations were analysed using the Spearman ρ correlation coefficient. Differences in pre- and postoperative parameters were compared using the paired Wilcoxon signed-rank test and the independent Mann−Whitney U test (for normally distributed variables). Values were considered statistically significant for $p < 0.05$. All statistical analyses were performed in R (R Foundation for Statistical Computing, Vienna, Austria).

3. Results

3.1. Patient population

A total of 31 patients were included in the analysis (18 males). Mean age at surgery was 2.3 ± 1.7 years (range 3 months−5.6 years). In all, 29 (94%) patients underwent SA-PVE for raised ICP, and 2 (6%) patients for improvement of head shape. Thickness measurement showed an average of 2.98 ± 0.82 mm. Average preoperative CI was $86.3 \pm 9.1\%$, and the average preoperative ICV was 1188.4 ± 255.9 cm^3. The preoperative ICV was not correlated with the preoperative CI ($\rho = 0$, $p = 0.98$). Table 1 displays a summary of included patients.

Successful surgery was reported for all cases. ICP normalisation, confirmed either by ophthalmology or by clinical evaluation, was achieved in all 29 patients who underwent SA-PVE for raised ICP. In the 2 patients who underwent SA-PVE for head shape improvement, results were described as satisfactory by the operating neurosurgeons.

3.2. Surgical parameters

From the total of 31 patients, six had a fully cut-through osteotomy ('flap', Fig. 3B), whereas in 25 patients, the flap remained attached to the occipital bone ('hinge', Fig. 3A). Mean age for the flap group was 3.3 ± 1.6, mean age for the hinge group was 2.0 ± 1.4 (no significant age difference was found; $p = 0.12$). Mean age for patients receiving two springs (n = 19) was 2.0 ± 1.5 years, and mean age for patients receiving more than two (four or six, n = 12) springs was 2.8 ± 1.9 years (no statistical difference was found; $p = 0.30$). Springs remained in situ for 282 ± 247 days.

3.3. Statistical shape modelling

The first 10 principal components accounted for 80% of the head shape variations in the population; the first principal component (PCA Mode 1; PC1) accounted for 32% of the differences. Fig. 7 displays the ± 2.7 SD of the head shapes in the first principal component.

PC1 had a positive correlation with the preoperative CI ($\rho = 0.66$, $p < 0.001$) (Fig. 8) and a negative correlation with age at time of surgery ($\rho = -0.73$, $p < 0.001$) and preoperative skull thickness ($\rho = -0.54$, $p = 0.0016$).

3.4. Surgical outcomes

Postoperatively, the average CI was $83.4 \pm 9.5\%$, with a decrease of $-2.9 \pm 4.3\%$ compared to preoperatively ($p < 0.001$). The average postoperative ICV was 1472.5 ± 232.5 cm^3, with an increase of 284.1 ± 171.6 cm^3 ($27.0 \pm 21.7\%$, $p < 0.001$). The postoperative ICV was not correlated with the postoperative CI ($\rho = 0.08$, $p = 0.66$), however, percentage change in ICV was significantly correlated with change in CI ($\rho = -0.38$, $p = 0.037$) (Fig. 9).

Correlations between main surgical outcomes and, respectively, patient demographics, surgical parameters and skull morphology described by SSM were calculated:

3.4.1. Surgical outcomes vs demographics

Age at surgery ($\rho = -0.60$, $p < 0.001$) and preoperative bone thickness ($\rho = -0.60$, $p < 0.001$) both showed negative significant correlations with percentage increase in ICV (Fig. 10). No correlation was found between change in CI and age at surgery or bone thickness.

Table 1
Characteristics of the patient population included in the study (N = 31).

Characteristic	No. of patients
Sex	
Male, n (%)	18 (58)
Female, n (%)	13 (42)
Patient diagnosis	
Apert	8
Bicoronal craniosynostosis	1
Cranial Dysraphism	1
Crouzon	9
Complex	9
ERF-related craniosynostosis	1
Muenke	1
Pfeiffer	1
Number of inserted springs	
2	19
4	9
6	3
Duration of spring insertion (months)	9.4 ± 8.2
Age at preoperative CT (years)	2.2 ± 2.1
Age at surgery (years)	2.3 ± 1.7
Age at postoperative CT (years)	3.3 ± 3.2
Time between preoperative CT and surgery (months)	1.6 ± 1.7
Time between surgery and postoperative CT (months)	11.8 ± 11.9
Time between preoperative and postoperative CT (months)	13.4 ± 16.5

K.R.R. Ramdat Misier, R.W.F. Breakey, L.S. van de Lande et al.

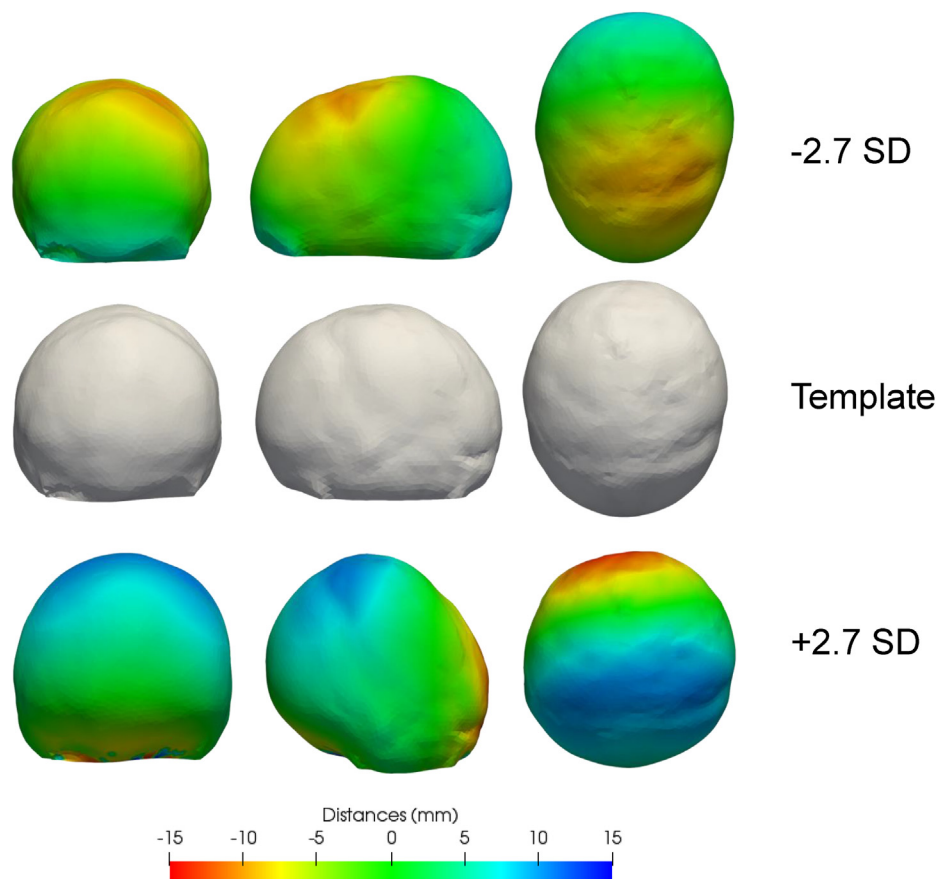*Journal of Cranio-Maxillo-Facial Surgery 50 (2022) 343–352*

Fig. 7. Head shapes of the first principal component. Frontal, side and top views of the −2.7 SD of the first principal component, the template and +2.7 SD of the first principal component PC1.

3.4.2. Surgical outcomes vs surgical parameters

An overview of the relationship between surgical outcomes and surgical parameters is displayed in Table 2. In analysing the number of springs used for the procedure (two springs vs four or six springs), no significant differences were seen between the two groups in terms of change in ICV ($p = 1.00$). Change in CI was more pronounced in the patient group receiving four to six springs; however, the difference did not reach statistical significance ($p = 0.07$). The type of surgical osteotomy ("flap" vs "hinge") showed no significant difference in terms of change in ICV ($p = 0.34$) and change in CI ($p = 0.50$). The duration of spring insertion did not show a significant correlation with the change in ICV ($\rho = 0.08$, $p = 0.66$) and the change in CI ($\rho = -0.14$, $p = 0.45$).

3.4.3. Surgical outcomes vs statistical shape modelling

The change in ICV ($\rho = 0.68$, $p < 0.001$, Fig. 11), as well as the percentage change in ICV ($\rho = 0.62$, $p < 0.001$) showed a significant correlation with PC1; however, the change in CI was not correlated with the first principal component.

4. Discussion

In this study, a group of patients who underwent SA-PVE for cranial augmentation was included, and population demographics, surgical parameters and surgical outcomes are summarised. SSM was used to generate a template head shape for the patient population and to capture the shape difference from the template for every individual patient. Correlations between surgical outcomes, population demographics, surgical parameters and PCA vectors
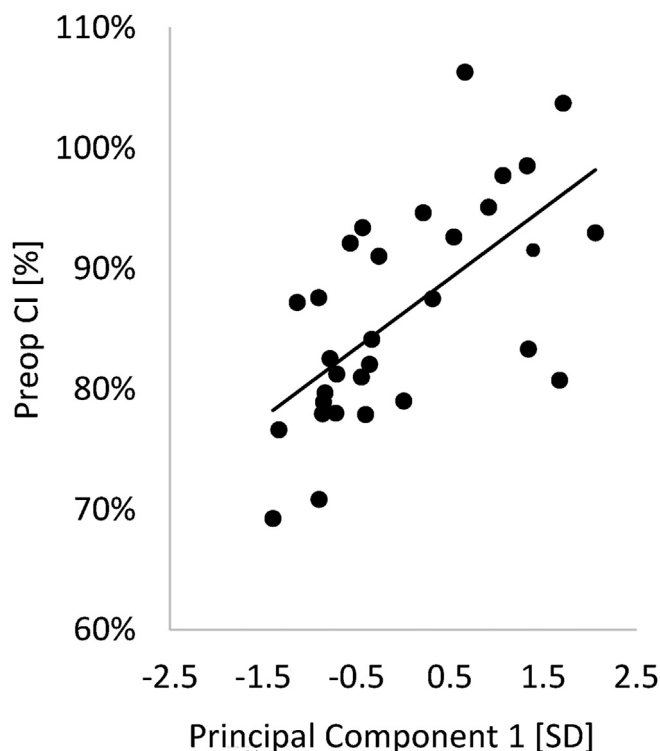

Fig. 8. Correlation plot for the first principal component (PC1) and the preoperative cranial index (CI).
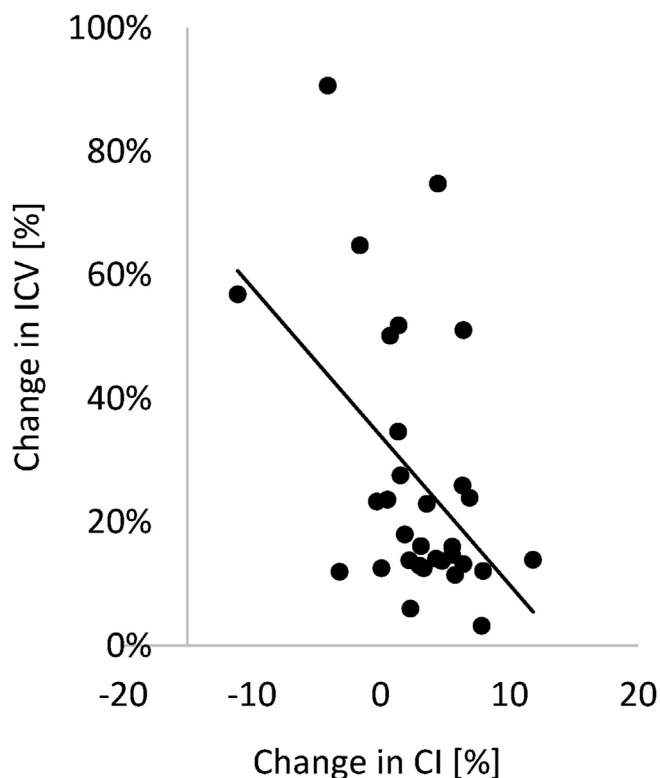
Fig. 9. Correlation plot for the change in cranial index (CI) and the change in intracranial volume (ICV).

Table 2
Characteristics and outcomes of patients receiving two and four or six springs; outcomes for patients with a 'flap' versus a 'hinge' osteotomy.

Characteristic	2	4 or 6	Difference
Age at surgery	2.0 ± 1.5	2.8 ± 1.9	$p = 0.30$
ICV change [cm^3]	291.8	271.9	$p = 1.00$
CI change [%]	-1.8 ± 4.3	-4.7 ± 3.7	$p = 0.07$
Type of osteotomy	Flap	Hinge	Difference
Age at surgery	3.3 ± 1.6	2.0 ± 1.4	$p = 0.12$
ICV change [cm^3]	209.4 ± 65.5	302.0 ± 184.9	$p = 0.34$
CI change [%]	3.3 ± 2.6	2.8 ± 4.7	$p = 0.50$

provided important information on factors that affect the extent of calvarial augmentation in this type of procedure.

PC1 showed significant correlations with CI, bone thickness and age at time of surgery. As volumes of 3D models were equal, there was no correlation between PC1 and preoperative ICV. By visualising the variation of PC1 in the range ±2.7 SD, it is clear how this parameter is related to head shape, varying from a more brachycephalic shape to a more normocephalic one. By combining this with the other parameters of the study, it can be inferred that higher values of the first principal component were correlated with younger, brachycephalic patients with a lower bone thickness. Higher values of PC1 also showed a correlation with a larger increase in ICV, indicating a relationship between patient's head shape and the volumetric outcomes after surgery: brachycephalic patients increased more in ICV. This was true for the absolute volumetric increase, as well as for percentage volumetric increase.

In this cohort, the change in CI was negatively correlated with the change in ICV; that is, a lower change in CI is connected to a higher change in ICV. Possibly, in SA-PVE patients with a higher volumetric increase, skull volume did not increase only posteriorly, but also bilaterally, resulting in a lower change in CI. In a previous study, Leikola et al. (Leikola et al., 2014) found poor correlations between the CI and ICV in non-syndromic scaphocephalic patients. The same trend was found in this study; therefore, a good aesthetic outcome in terms of CI decrease may be connected with an unsatisfactory volumetric change, and a balance should be sought.

The correlation between change in ICV and preoperative bone thickness suggests that for optimal volume increase, not only the age, but also calvarial maturity should be monitored. This is in line with a previous study from Rodriguez-Florez et al., in which the authors advised on monitoring of calvarial maturity in spring-assisted surgery for sagittal synostosis (Rodriguez-Florez et al., 2017c).

When the number of implanted springs was analysed, data showed that insertion of more than two springs did not show better outcomes in terms of change in ICV and CI. The duration of spring insertion was not correlated with different changes in ICV or CI. As hypothesized by Borghi et al. the calvarium accommodates the mechanical action of springs because of the inherent viscoelasticity of the paediatric skull (Borghi et al., 2017). This may explain why
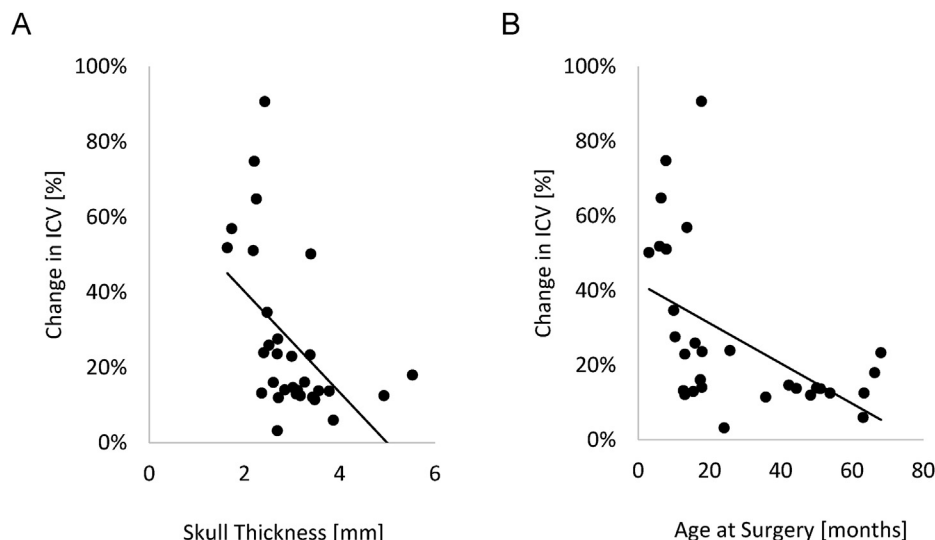

Fig. 10. A: Correlation plot for skull thickness and change in intracranial volume (ICV). B: Correlation plot for age at surgery and change in ICV.
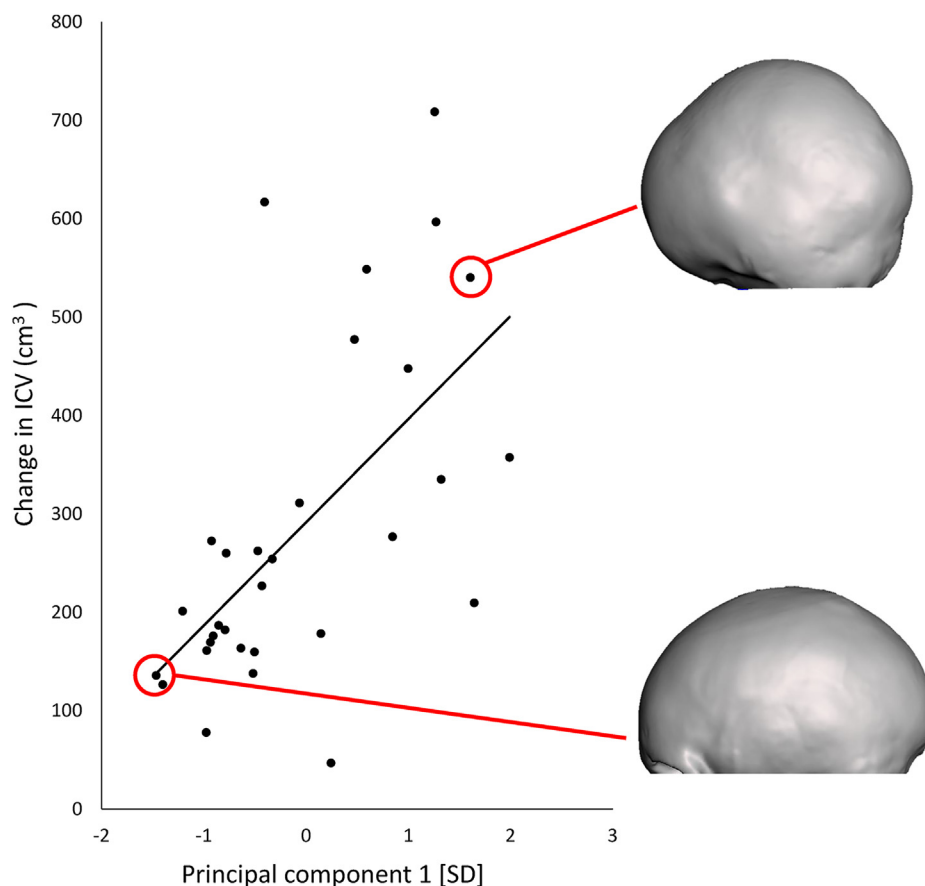
Fig. 11. Correlation plot for the first principal component (PC1) and the change in intracranial volume. Example models are shown for the patients with high (upper model) and low (lower model) PC1 values.

the amount of force exerted does not have an effect on the final amount of distraction achieved. A similar conclusion was achieved by Sun et al., who concluded that the number of springs implanted did not affect cranial reshaping in the correction of sagittal craniosynostosis (Sun et al., 2018).

When type of osteotomy was assessed, both 'flap' and 'hinge' osteotomies seemed to result in similar outcomes in terms of ICV and CI change. The choice to create a complete 'flap' after the osteotomy and to attach this piece of bone with metal wires is based mostly on the patient's age and the malleability of the calvarium. Although not significant, the 'flap' group did show a higher average age at time of surgery. Thus, the similar results between the two groups might be based on adequate adaptation of the osteotomy per patient.

Our results show that head shape plays an important role on the extent of calvarial augmentation, along with calvarial maturity (skull thickness) and age at surgery. Such correlation was a result of the combination of non-parametric SSM and PCA. PCA is a well-known tool used to describe craniofacial anomalies. Maas et al. used PCA to describe midfacial deformities in patients craniofacial microsomia (Maas et al., 2018). Moreover, Pluijmers et al. and Staal et al. used PCA to describe skull deformities in Apert and Crouzon-Pfeiffer patients, respectively (Pluijmers et al., 2012; Staal et al., 2015). The combination of SSM and PCA has also been used before in craniofacial surgery. Rodriguez-Florez et al. previously used this combination to quantify the aesthetic effects of surgical correction of trigonocephaly (Rodriguez-Florez et al., 2017b). The main novelty of the current study, next to the focus on SA-PVE, was

to use SSM and PCA for describing preoperative head shape variations and correlate these to the change in ICV.

In the current study, models for SSM and PCA were derived from CT scans, which were performed for clinical indications. 3D CT scans are commonly used in the field of craniofacial surgery (Han et al., 2019; Prevost et al., 2019; Rodriguez-Florez et al., 2019; Sunaga et al., 2019). However, because of CT-related radiation exposure, the number of CT scans performed in children should be limited (Wilbrand et al., 2012; Almohiy, 2014; Prevost et al., 2019). Fortunately, 3D models used to carry out SSM and PCA do not have to be derived from CT scans. Non-radiative, 3D-stereo-photogrammetry imaging techniques have proven to accurately capture (craniosynostosis) patients head shapes and can be used interchangeably with traditional anthropometric measurements and CT scans (McKay et al., 2010; Wilbrand et al., 2012; Tenhagen et al., 2016; Beaumont et al., 2017; Klausing et al., 2019). Methods employed in the current study can be used on 3D-photogrammetry images as well. We believe that in the future, most head shape analyses will be performed using images derived from 3D-photogrammetry, and we hope our study contributes to this trend.

The effectiveness of SA-PVE in the treatment of multisuture craniosynostosis has been proved before by De Jong et al. The authors reported a superior increase in skull circumference and increase in anterior ± posterior length, compared to those achieved with the conventional PVE technique (De Jong et al., 2013). In the current study, in which a similar surgical technique was used, we can expand these findings by reporting the increase in ICV and decrease in CI in patients with multisuture craniosynostosis. Tovjetjarn et al. studied the change in ICV after spring-assisted

cranioplasty in patients with bilateral coronal synostosis. The authors reported post-surgical volumetric changes comparable to growth in normal children (Tovetjärn et al., 2014). Compared to the current study, Tovjetjarn et al. used a slightly different technique, by combining spring-assisted distraction with remodelling of the forehead. Springs were sometimes placed over intact, i.e. non-osteomized, lambdoid sutures, which may limit the spring's expanding capabilities (Tovetjarn et al., 2012). In our study, the springs were always placed between osteotomized bone.

The most common alternative for SA-PVE is posterior cranial vault distraction, a technique in which PVE is combined with distraction osteogenesis (PVDO). Multiple studies have reported the change in intracranial volume for posterior cranial vault distraction (Serlo et al., 2011; Derderian et al., 2015; Shimizu et al., 2016; Rocco et al., 2018; Senda et al., 2019). Increases in ICV are similar between distractors and springs.

Even though the ICV does not directly provide information about the ICP, it is still an important outcome of calvarial surgery and is thus reported frequently. However, special attention had to be paid to the use and comparison of the ICV measurements. First, a wide range of time span between pre- and postoperative CT scans was observed. This was the result of limited use of CT scans, in an attempt to minimalize radiation exposure in young children. Second, an increase in ICV may not be attributed solely to SA-PVE, as normal calvarial growth will contribute to this as well, especially in young patients. A previous study by Derderian et al. described the difficulty of comparing ICV changes during a time of rapid calvarial growth for syndromic children. Due to the lack of normative data on volumetric change in syndromic craniosynostosis available at that time, the authors compared their results on volumetric changes after PVDO to volumes in healthy infants (Derderian et al., 2015). To deal with these limitations, we adjusted the ICV values for each patient to the day of surgery and to one year after surgery. Numerical adjustments were based on syndrome-specific ICV growth curves published by Breakey et al. (Breakey et al., 2018). By adjusting the ICV, we dealt with time differences between CT scans, and ensured that a uniform time period of calvarial growth was considered, allowing for more accurate comparisons between patients. Nevertheless, these factors cannot be corrected for completely and should be taken into account when interpreting the results.

The current results may be clinically relevant in predicting surgical outcomes for patients undergoing SA-PVE: surgeons could use the results as an indication of what volumetric increase to expect from specific patients by calculating new patient shape vectors and comparing them with those of the current PVE population; change in shape or volume could then be estimated by using regression techniques such as partial least square, which combines PCA dimensionality reduction with linear regression techniques (Mansi et al., 2011). In case of head shapes which correlated with limited ICV increase, the risk of recurrence of raised ICP could be addressed more accurately.

5. Conclusion

Spring-assisted posterior vault expansion is an effective method of increasing the intracranial volume and resolving raised intracranial pressure in children with syndromic and complex craniosynostosis. Younger, markedly brachycephalic head shapes show higher volumetric increases and may thus benefit more from surgery. We recommend monitoring of skull bone thickness to achieve optimal intracranial volume expansion, as skull bone thickness seems to be a crucial factor in the amount of expansion that can be achieved. Insertion of more than two springs or performing a fully cut-through osteotomy does not seem to have an impact on

volumetric increase and can be adjusted according to specific cases. Normal calvarial growth should be taken into account when interpreting volumetric increases, to avoid overestimation of volumetric increases. The results presented could be clinically incorporated in assessing outcomes related to specific head shapes.

Declaration of competing interest

N.U. Owase Jeelani acts as a consultant for the KLS Martin group.

References

Almohiy, H., 2014. Paediatric computed tomography radiation dose: a review of the global dilemma. World J. Radiol. 6 (1).

Antiga, L., Piccinelli, M., Botti, L., Ene-Iordache, B., Remuzzi, A., Steinman, D.A., 2008. An image-based modeling framework for patient-specific computational hemodynamics. Med. Biol. Eng. Comput. 46, 1097.

Beaumont, C.A.A., Knoops, P.G.M., Borghi, A., Jeelani, N.U.O., Koudstaal, M.J., Schievano, S., Dunaway, D.J., Rodriguez-Florez, N., 2017. Three-dimensional surface scanners compared with standard anthropometric measurements for head shape. J. Cranio-Maxillo-Fac. Surg. 45, 921–927.

Borghi, A., Schievano, S., Rodriguez Florez, N., McNicholas, R., Rodgers, W., Ponniah, A., James, G., Hayward, R., Dunaway, D., Jeelani, N.U.O., 2017. Assessment of spring cranioplasty biomechanics in sagittal craniosynostosis patients. J. Neurosurg. Pediatr. 20, 400–409.

Bouaoud, J., Hennocq, Q., Paternoster, G., James, S., Arnaud, E., Khonsari, R.H., 2020. Excessive ossification of the bandeau in Crouzon and Apert syndromes. J. Cranio-Maxillo-Fac. Surg. 48, 376–382.

Breakey, R.W.F., Knoops, P.G.M., Borghi, A., Rodriguez-Florez, N., O'Hara, J., James, G., Dunaway, D.J., Schievano, S., Jeelani, N.U.O., 2018. Intracranial volume and head circumference in children with unoperated syndromic craniosynostosis. Plast. Reconstr. Surg. 142, 708e–717e.

Breakey, W., Knoops, P.G.M., Borghi, A., Rodriguez-Florez, N., Dunaway, D.J., Schievano, S., Jeelani, O.N.U., 2017. Intracranial volume measurement: a systematic review and comparison of different techniques. J. Craniofac. Surg. 28, 1746–1751.

Czerwinski, M., Kolar, J.C., Fearon, J.A., 2011. Complex craniosynostosis. Plast. Reconstr. Surg. 128, 955–961.

De Jong, T., Van Veelen, M.L.C., Mathijssen, I.M.J., 2013. Spring-assisted posterior vault expansion in multisuture craniosynostosis. Childs Nerv. Syst. 29, 815–820.

Derderian, C.A., Wink, J.D., McGrath, J.L., Collinsworth, A., Bartlett, S.P., Taylor, J.A., 2015. Volumetric changes in cranial vault expansion: comparison of fronto-orbital advancement and posterior cranial vault distraction osteogenesis. Plast. Reconstr. Surg. 135, 1665–1672.

Durrleman, S., Prastawa, M., Charon, N., Korenberg, J.R., Joshi, S., Gerig, G., Trouvé, A., 2014. Morphometry of anatomical shape complexes with dense deformations and sparse parameters. Neuroimage 101, 35–49.

Han, W., Yang, X., Wu, S., Fan, S., Chen, X., Aung, Z.M., Liu, T., Zhang, Y., Gu, S., Chai, G., 2019. A new method for cranial vault reconstruction: augmented reality in synostotic plagiocephaly surgery. J. Cranio-Maxillo-Fac. Surg. 47, 1280–1284.

Johnson, D., Wilkie, A.O.M., 2011. Craniosynostosis. Eur. J. Hum. Genet. 19, 369.

Jolliffe, I., 2002. Principal component analysis. In: Lovric, M. (Ed.), International Encyclopedia of Statistical Science. Springer, Berlin.

Khonsari, R.H., Haber, S., Paternoster, G., Fauroux, B., Morisseau-Durand, M.-P., Cormier-Daire, V., Legeai-Mallet, L., James, S., Hennocq, Q., Arnaud, E., 2020. The influence of fronto-facial monobloc advancement on obstructive sleep apnea: an assessment of 109 syndromic craniosynostoses cases. J. Cranio-Maxillo-Fac. Surg. 48, 536–547.

K.R.R. Ramdat Misier, R.W.F. Breakey, L.S. van de Lande et al.

Journal of Cranio-Maxillo-Facial Surgery 50 (2022) 343–352

Kim, S.Y., Choi, J.W., Shin, H.J., Lim, S.Y., 2019. Reliable manifestations of increased intracranial pressure in patients with syndromic craniosynostosis. J. Cranio-Maxillo-Fac. Surg. 47, 158–164.

Klausing, A., Röhrig, A., Lüchters, G., Vogler, H., Martini, M., 2019. Follow-up study to investigate symmetry and stability of cranioplasty in craniosynostosis–introduction of new pathology-specific parameters and a comparison to the norm population. J. Cranio-Maxillo-Fac. Surg. 47, 1441–1448.

Kolar, J.C., Salter, E.M., 1997. Craniofacial Anthropometry: Practical Measurement of the Head and Face for Clinical, Surgical, and Research Use. Charles C. Thomas Publisher, Springfield, IL.

Lehner, M., Ferrari-von Klot, F., Zundel, S., Wendling-Keim, D., 2019. Osteoclastic craniectomy for scaphocephaly in infants results in physiological head shapes. J. Cranio-Maxillo-Fac. Surg. 47, 1891–1897.

Leikola, J., Koljonen, V., Heliövaara, A., Hukki, J., Koivikko, M., 2014. Cephalic index correlates poorly with intracranial volume in non-syndromic scaphocephalic patients. Childs Nerv. Syst. 30, 2097–2102.

Maas, B.D.P.J., Pluijmers, B.I., Knoops, P.G.M., Ruff, C., Koudstaal, M.J., Dunaway, D., 2018. Using principal component analysis to describe the midfacial deformities in patients with craniofacial microsomia. J. Cranio-Maxillo-Fac. Surg. 46, 2032–2041.

Mansi, T., Voigt, I., Leonardi, B., Pennec, X., Durrleman, S., Sermesant, M., Delingette, H., Taylor, A.M., Boudjemline, Y., Pongiglione, G., Ayache, N., 2011. A statistical model for quantification and prediction of cardiac remodelling: application to tetralogy of Fallot. IEEE Trans. Med. Imag. 30, 1605–1616.

McKay, D.R., Davidge, K.M., Williams, S.K., Ellis, L.A., Chong, D.K., Teixeira, R.P., Greensmith, A.L., Holmes, A.D., 2010. Measuring cranial vault volume with three-dimensional photography: a method of measurement comparable to the gold standard. J. Craniofac. Surg. 21, 1419–1422.

O'Hara, J., Way, B., Borghi, A., Knoops, P.G.M., Chua, D., Hayward, R.D., 2019. The turricephaly index: a validated method for recording turricephaly and its natural history in Apert syndrome. J. Cranio-Maxillo-Fac. Surg. 47, 414–419.

Pluijmers, B.I., Ponniah, A.J.T., Ruff, C., Dunaway, D., 2012. Using principal component analysis to describe the Apert skull deformity and simulate its correction. J. Plast. Reconstr. Aesthetic Surg. 65, 1750–1752.

Prevost, R., Keribin, P., Batut, C., Guichard, B., Ambroise, B., Bohra, A., Benateau, H., Veyssiere, A., 2019. Management of non-syndromic craniosynostoses in France in 2015: a national survey. J. Cranio-Maxillo-Fac. Surg. 47, 556–560.

Renier, D., Lajeunie, E., Arnaud, E., Marchac, D., 2000. Management of craniosynostoses. Childs Nerv. Syst. 16, 645–658.

Rocco, F.D., Usami, K., Protzenko, T., Collet, C., Giraudat, K., Arnaud, E., 2018. Results and limits of posterior cranial vault expansion by osteotomy and internal distractors. Surg. Neurol. Int. 9, 217.

Rodgers, W., Glass, G.E., Schievano, S., Borghi, A., Rodriguez-Florez, N., Tahim, A., Angullia, F., Breakey, W., Knoops, P., Tenhagen, M., O'Hara, J., Ponniah, A., James, G., Dunaway, D.J., Jeelani, N.U.O., 2017. Spring-assisted cranioplasty for the correction of nonsyndromic scaphocephaly: a quantitative analysis of 100 consecutive cases. Plast. Reconstr. Surg. 140, 125–134.

Rodriguez-Florez, N., Bruse, J.L., Borghi, A., Vercruysse, H., Ong, J., James, G., Pennec, X., Dunaway, D.J., Jeelani, N.U.O., Schievano, S., 2017a. Statistical shape modelling to aid surgical planning: associations between surgical parameters and head shapes following spring-assisted cranioplasty. Int. J. Comput. Assist. Radiol. Surg. 12, 1739–1749.

Rodriguez-Florez, N., Florez-Tapia, A., Jeelani, N.U.O., Schievano, S., Dunaway, D.J., Hayward, R.D., 2019. Investigating the cause of late deformity following fronto-orbital remodelling for metopic synostosis using 3D CT imaging. J. Cranio-Maxillo-Fac. Surg. 47, 170–178.

Rodriguez-Florez, N., Göktekin, Ö.K., Bruse, J.L., Borghi, A., Angullia, F., Knoops, P.G.M., Tenhagen, M., O'Hara, J.L., Koudstaal, M.J., Schievano, S., Jeelani, N.U.O., James, G., Dunaway, D.J., 2017b. Quantifying the effect of corrective surgery for trigonocephaly: a non-invasive, non-ionizing method using three-dimensional handheld scanning and statistical shape modelling. J. Cranio-Maxillo-Fac. Surg. 45, 387–394.

Rodriguez-Florez, N., Ibrahim, A., Hutchinson, J.C., Borghi, A., James, G., Arthurs, O.J., Ferretti, P., Dunaway, D., Schievano, S., Jeelani, N.U.O., 2017c. Cranial bone structure in children with sagittal craniosynostosis: relationship with surgical outcomes. J. Plast. Reconstr. Aesthetic Surg. 70, 1589–1597.

Rtshiladze, M.A., Roy, A.-A., Goltsman, D., Hunt, J., Reddy, R., Gianoutsos, M.P., 2019. The removal of cranial springs used in the treatment of scaphocephaly: a minimal access approach. J. Cranio-Maxillo-Fac. Surg. 47, 1706–1711.

Senda, D., Orgun, D., Shimizu, A., Shimoji, K., Miyajima, M., Arai, H., Mizuno, H., Komuro, Y., 2019. Quantitative analysis of change in intracranial volume after posterior cranial vault distraction and frontal orbital advancement/remodeling. J. Craniofac. Surg. 30, 23–27.

Serlo, W.S., Ylikontiola, L.P., Lähdesluoma, N., Lappalainen, O.-P., Korpi, J., Verkasalo, J., Sàndor, G.K.B., 2011. Posterior cranial vault distraction osteogenesis in craniosynostosis: estimated increases in intracranial volume. Childs Nerv. Syst. 27, 627–633.

Sgouros, S., Goldin, J.H., Hockley, A.D., Wake, M.J.C., 1996. Posterior skull surgery in craniosynostosis. Childs Nerv. Syst. 12, 727–733.

Shimizu, A., Komuro, Y., Shimoji, K., Miyajima, M., Arai, H., 2016. Quantitative analysis of change in intracranial volume after posterior cranial vault distraction. J. Craniofac. Surg. 27, 1135–1138.

Staal, F.C.R., Ponniah, A.J.T., Angullia, F., Ruff, C., Koudstaal, M.J., Dunaway, D., 2015. Describing Crouzon and Pfeiffer syndrome based on principal component analysis. J. Cranio-Maxillo-Fac. Surg. 43, 528–536.

Sun, J., Ter Maaten, N.S., Mazzaferro, D.M., Wes, A.M., Naran, S., Bartlett, S.P., Taylor, J.A., 2018. Spring-mediated cranioplasty in sagittal synostosis: does age at placement affect expansion? J. Craniofac. Surg. 29, 632–635.

Sunaga, A., Sugawara, Y., Gomi, A., Chi, D., Kamochi, H., Uda, H., Yoshimura, K., 2019. Multidirectional cranial distraction osteogenesis technique for treating bicoronal synostosis. J. Cranio-Maxillo-Fac. Surg. 47, 1436–1440.

Taylor, W.J., Hayward, R.D., Lasjaunias, P., Britto, J.A., Thompson, D.N.P., Jones, B.M., Evans, R.D., 2001. Enigma of raised intracranial pressure in patients with complex craniosynostosis: the role of abnormal intracranial venous drainage. J. Neurosurg. 94, 377.

Tenhagen, M., Bruse, J.L., Rodriguez-Florez, N., Angullia, F., Borghi, A., Koudstaal, M.J., Schievano, S., Jeelani, O., Dunaway, D., 2016. Three-dimensional handheld scanning to quantify head-shape changes in spring-assisted surgery for sagittal craniosynostosis. J. Craniofac. Surg. 27, 2117–2123.

Tovetjarn, R., Maltese, G., Kolby, L., Kreiborg, S., Tarnow, P., 2012. Spring-assisted cranioplasty for bicoronal synostosis. J. Craniofac. Surg. 23, 977–981.

Tovetjärn, R.C., Maltese, G., Wikberg, E., Bernhardt, P., Kölby, L., Tarnow, P.E., 2014. Intracranial volume in 15 children with bilateral coronal craniosynostosis. Plast. Reconstr. Surg. Glob. Open 2, e243.

Wiberg, A., Magdum, S., Richards, P.G., Jayamohan, J., Wall, S.A., Johnson, D., 2012. Posterior calvarial distraction in craniosynostosis–an evolving technique. J. Cranio-Maxillo-Fac. Surg. 40, 799–806.

Wilbrand, J.-F., Szczukowski, A., Blecher, J.-C., Pons-Kuehnemann, J., Christophis, P., Howaldt, H.-P., Schaaf, H., 2012. Objectification of cranial vault correction for craniosynostosis by three-dimensional photography. J. Cranio-Maxillo-Fac. Surg. 40, 726–730.